Tunable negative and positive coercivity for SmCo/(Co/Gd) exchange springs investigated with SQUID magnetometry

S. Demirtas,[1] M. R. Hossu,[2] M. Arikan,[2] A. R. Koymen,[2] and M. B. Salamon[1]
[1]*Department of Physics, University of Texas at Dallas, Richardson, Texas 75083, USA*
[2]*Department of Physics, University of Texas at Arlington, Arlington, Texas 76019, USA*
(Received 11 July 2007; revised manuscript received 18 September 2007; published 27 December 2007)

Temperature dependent static magnetic properties of Co/Gd multilayers, grown on SmCo, are experimentally investigated by means of SQUID magnetometry. The SmCo/(Co/Gd) system shows an exchange spring behavior above the compensation temperature (T_{comp}) at which the magnetization of the antiferromagnetically coupled multilayer is zero. Below T_{comp}, a tunable negative coercivity state (inverse hysteresis) appears, due to the coupling between the hard SmCo and soft Co/Gd multilayers, irrespective of whether Co or Gd is proximate to the SmCo. However, for the strongly ferromagnetically coupled Co interface layer, negative coercivity persists over a larger temperature interval. The negative coercivity state vanishes if the coercivity of the SmCo layer is increased by controlling the Cu underlayer thickness.

DOI: 10.1103/PhysRevB.76.214430 PACS number(s): 75.70.Cn, 75.50.Gg, 75.50.Vv

Exchange spring magnets have been studied for over 20 years, driven by the need for smaller bit sizes with higher energy product and for permanent magnet applications.[1,2] An exchange spring magnet combines the high magnetization of a soft magnet with a coercively hard one. For example, the soft layer can be among the transition metals or their alloys (Fe, Co, Ni, Py, etc.) and the hard layer is generally SmCo or NdFeB. The spring behavior is due to the ferromagnetic coupling at the interface between hard and soft layers.[3–14]

In this study, we selected SmCo as the hard magnet and a ferrimagnetic Co/Gd multilayer as the soft layer, with the thickness of the soft layer larger than that of the hard SmCo layer. The layer thicknesses of the Co/Gd multilayers are regulated such that the compensation temperature (T_{comp}), where Gd and Co magnetizations are equal, occurs in the temperature range of interest (10–300 K). Therefore, we can analyze the exchange spring behavior, when the Co subnetwork between the SmCo and Co/Gd multilayer is either aligned ferromagnetically (Co dominant) or antiferromagnetically (Gd dominant) at saturation depending on T relative to T_{comp}. The problem we address is whether strong coupling exists at the interface between SmCo and Co/Gd multilayers and, if so, its effect on the rest of the multilayer. Would it be like the standard exchange spring behavior? The answer is positive for $T > T_{comp}$. However, interesting physics emerges below T_{comp}. We will show that ferromagnetic coupling at the interface with SmCo works against the switching of the soft layer magnetization above T_{comp}, while antiferromagnetic alignment below T_{comp} eases the rotation, making it coercively soft. We will show that the coercivity can be tuned to be negative below T_{comp}.

There are examples of exchange-coupled hard/soft systems in literature[15,16] which show an exchange spring behavior both at high and low external fields. For example, $DyFe_2/YFe_2$ combinations exhibit a peculiar behavior when the interface coupling is antiferromagnetic (which corresponds to the configuration below T_{comp} in our case). Proposed exchange spring behavior at high fields is very similar to the twisted states[17,18] for the ferrimagnetic Fe/Gd (and Co/Gd) multilayers; the twist penetrates also into the hard layer. The spring motion of the soft YFe_2 layer is controlled by the type of interface coupling with the hard $DyFe_2$ layer. The coupling and orientation can be regulated by the composition (or as shown in this paper by temperature).

Samples were prepared in a dc magnetron sputtering system at room temperature. The unbaked base pressure of the UHV deposition chamber was 10^{-9} Torr. Ultrahigh purity argon gas was used and the deposition pressure was 3 mTorr. Samples were deposited on Corning glass substrates and either 100 or 1000 Å thick Cu layers were used as buffer underlayers in all samples. A quartz thickness gauge, calibrated by a stylus profilometer, monitored the deposition thicknesses *in situ*. The $Sm_{0.17}Co_{0.83}$ alloy, which is close to the $SmCo_5$ composition, was created by codeposition from pure Co and Sm targets. Bilayers of Co and Gd were repeated 16 times to form the multilayer. Approximately 25 thin film samples were grown. Structural characterization was done using an x-ray diffractometer. Magnetic measurements are made using a SQUID magnetometer between 10 and 350 K.

The x-ray diffraction pattern for the SmCo 300 Å/Cu 100 Å/glass is shown in Fig. 1(a). Neither the SmCo nor Cu has a preferred orientation; the SmCo alloy can be consid-

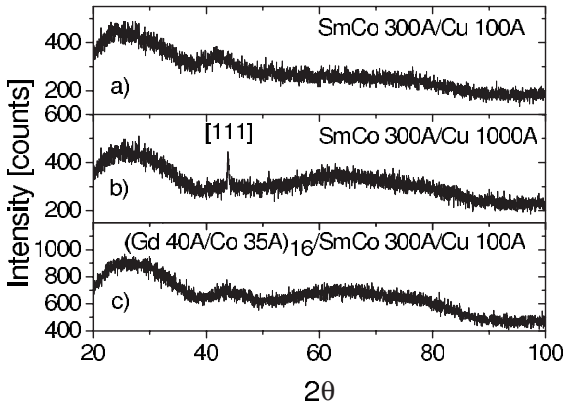

FIG. 1. X-ray diffraction pattern for the (a) SmCo 300 Å/Cu 100 Å, (b) SmCo 300 Å/Cu 1000 Å, and (c) $(Gd\ 40\ Å/Co\ 35\ Å)_{16}$/SmCo 300 Å/Cu 100 Å films.

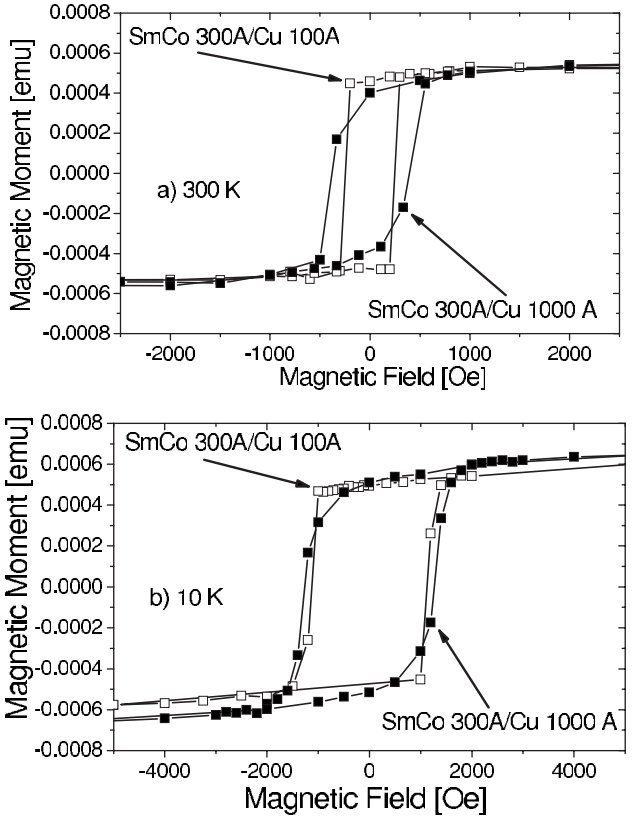

FIG. 2. Hysteresis loops for the SmCo 300 Å/Cu 1000 Å and SmCo 300 Å/Cu 100 Å films at (a) 300 K and (b) 10 K. The difference in saturation moment between the two samples results from different sample areas.

ered as polycrystalline. In contrast, x-ray data for the SmCo grown on thick Cu underlayer show a preferred orientation. As shown in Fig. 1(b), SmCo 300 Å/Cu 1000 Å/glass has a [111] texture for Cu in the growth direction. As shown in Fig. 1(c), multilayers of Co and Gd at this thickness level (35–40 Å) grown on 100 Å Cu do not show any preferred texture and remain polycrystalline.

In Fig. 2, hysteresis curves for the 300 Å SmCo films, grown on 100 and 1000 Å thick Cu underlayers, are shown at 10 and 300 K. The 300 Å SmCo film, grown on a thicker Cu underlayer (1000 Å), has a higher coercivity throughout the entire temperature range than the one grown on a thinner (100 Å) Cu underlayer. The coercivity of the SmCo 300 Å/Cu 1000 Å film is on the order of 400 Oe at room temperature and approximately 1250 Oe at 10 K, whereas that of the SmCo 300 Å/Cu 100 Å film shows smaller values, approximately 250 Oe at room temperature and 1100 Oe at 10 K. The difference of nearly 150 Oe throughout the entire temperature range of measurement is consistent with the structural data, where thicker underlayers of Cu can establish a proper [111] texture, while a thin Cu underlayer lacks any preferred orientation on the glass substrate. It has been shown in the literature[19–26] that growing SmCo on thick Cu increases the coercivity. Higher coercivity may mean more grain boundaries or more pinning sites that keep the SmCo domain walls from sweeping freely through the

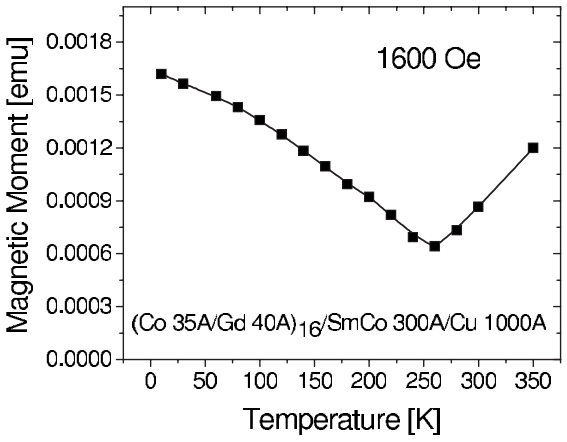

FIG. 3. Magnetic moment as a function of temperature for the (Co 35 Å/Gd 40 Å)$_{16}$/SmCo 300 Å/Cu 1000 Å system.

film. Although the aim of this study is not to increase the coercivity of SmCo, we will make use of this small difference in coercivity to understand the magnetic properties of the hard/soft combinations studied.

In Fig. 3, the magnetic moment of the (Co 35 Å/Gd 40 Å)$_{16}$/SmCo 300 Å/Cu 1000 Å system in a 1.6 kOe external magnetic field is shown as a function of temperature. The compensation temperature (T_{comp}) of this ferrimagnetic system is found to be approximately 250 K at this field, where the total moment has a minimum (the corresponding hysteresis loops are shown at Fig. 7). Above T_{comp}, the larger Co moments are aligned at saturation with the external magnetic field and the smaller Gd moments are opposite (Co aligned); below T_{comp}, the magnetic orientation is reversed, with the larger Gd moment in the field direction and smaller Co moments opposed (Gd aligned).[27–44] When the SmCo layer is added to the Co/Gd multilayer to form the SmCo/(Co/Gd) system, SmCo spins are in the field direction at saturation irrespective of T_{comp}. Therefore, the nonvanishing vertical offset of magnetic moment at T_{comp} is due to the rigid magnetic moment of the SmCo layer. The amount of vertical shift in Fig. 3 is approximately 6×10^{-4} emu, which is consistent with Fig. 2. The external magnetic field was purposefully set to 1.6 kOe where the combined system is free of magnetic thermal hysteresis and twisted state effects for the Co/Gd multilayer.[27]

Note that the magnetic field required to suppress thermal hysteresis effects[27] nearly doubles compared to single Co/Gd multilayers, due to the enhanced uniaxial anisotropy with the addition of the hard SmCo layer. Although it does not affect the results presented here, we should emphasize that T_{comp} also depends on the nature of the system. As shown in Figs. 3, 4, 6, and 7, the films where Gd layer was grown first on SmCo have higher T_{comp} than those where the Co layer was grown first. Here, the Co/Gd multilayers have the same thicknesses with the deposition order reversed. While we cannot justify this observation based on the structural data shown in Fig. 1, it is possible that there is a proximity enhancement of the Gd magnetization by the SmCo underlayer. Indeed, the addition of the SmCo layer has the effect of increasing T_{comp} independent of whether the Co or Gd layer was grown first.

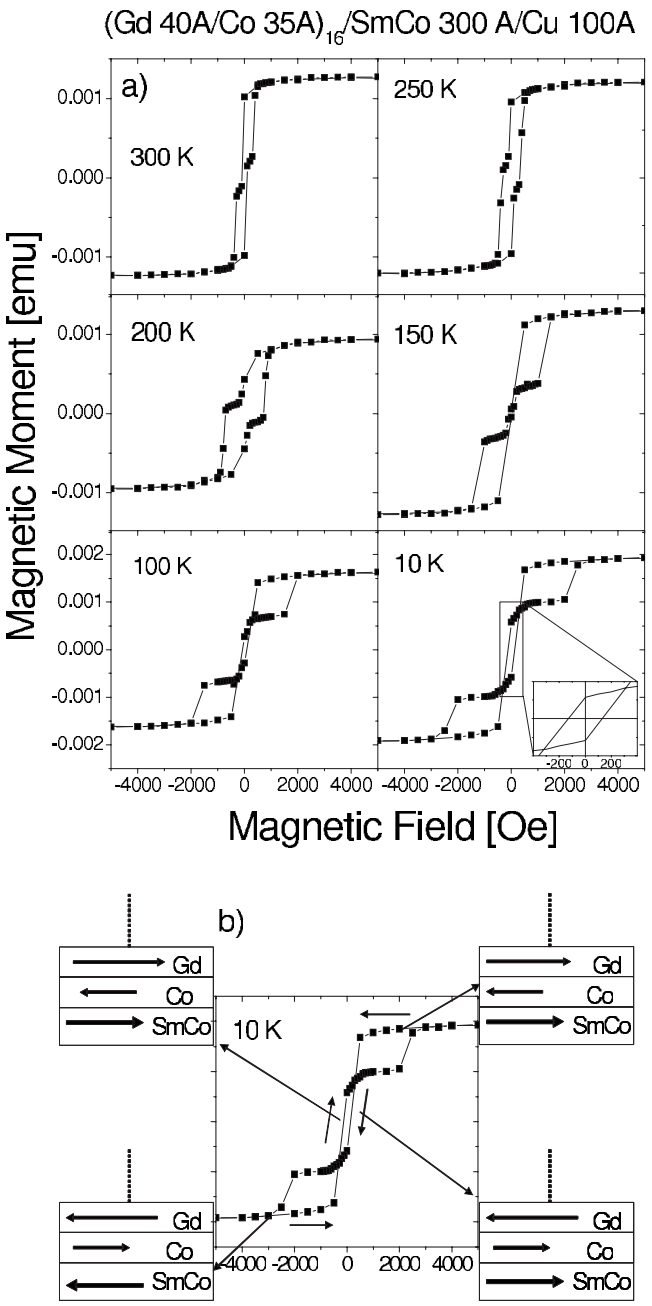

FIG. 4. (a) Selected hysteresis loops as a function of temperature for the (Gd 40 Å/Co 35 Å)$_{16}$/SmCo 300 Å/Cu 100 Å system. Inset shows the amount of negative coercivity. (b) Magnetic configurations at various points on the hysteresis loop at 10 K for the same film.

The temperature dependence of the hysteresis loops for the (Gd 40 Å/Co 35 Å)$_{16}$/SmCo 300 Å/Cu 100 Å multilayer, where the first layer adjacent to the SmCo layer is Co, is shown in Fig. 4(a). A hard/soft exchange spring behavior is observed only above T_{comp} (250–300 K) where the Co-aligned moment of the soft Co/Gd multilayer has a spring motion with respect to the harder SmCo layer. Here, the Gd moment is antiparallel to Co and SmCo layers at saturation. The exchange spring behavior is minimal because the coercivity of the SmCo alloy that we fabricated is on the order of

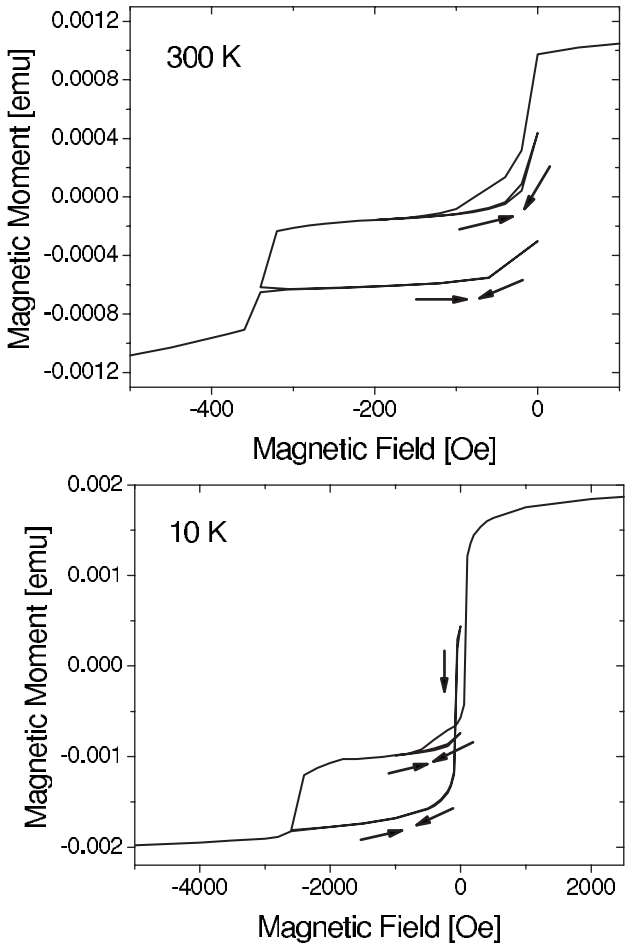

FIG. 5. Minor-loop demagnetization curves for the (Gd 40 Å/Co 35 Å)$_{16}$/SmCo 300 Å/Cu 100 Å system at (a) 300 K and (b) 10 K.

250 Oe, whereas the coercivity of the Co/Gd multilayer is around 100 Oe by itself at room temperature.[27]

To confirm the spring motion, we measured the demagnetization curves above and below T_{comp}. Reversible minor loops are shown in Fig. 5 on the irreversible portion of the hysteresis. To test the spring behavior, we strictly follow the standard procedure.[13] The magnetic field is cycled between 120 and 340 Oe to zero, as shown in Fig. 5(a). The recoil permeability is high and has a curvature comparable to a conventional single ferromagnetic phase magnet, as suggested by Kneller and Hawig.[13] However, as shown in Fig. 5(b), the spring motion cannot be confirmed below T_{comp} since the reversible minor loop measured between 2.6 and 0 kOe crosses the minor loop measured between 1 kOe and zero. The reversible minor loop, measured between 2.6 kOe and zero, resembles part of the major loop rather than a consequence of the spring mechanism. Although that loop crosses the other minor loop in Fig. 5(b), it has very high permeability and curvature, resembling more exchange spring behavior than that of a conventional magnet. However, the dynamics here are very much different from conventional exchange springs because there is antiferromagnetic coupling at the interface between SmCo and Co/Gd

layers below T_{comp}. Therefore, exchange spring behavior is confirmed only above T_{comp}.

As shown in Figs. 4(a) and 4(b), the orientation of the moments below T_{comp} is the reverse of the configuration above T_{comp}, that is, the Gd and SmCo moments are parallel at saturation and Co is antiparallel. We observe negative coercivity states between 10 and 100 K which are also called inverted hysteresis loops. This behavior differs from the exchange spring behavior above T_{comp}, in that the ferromagnetic interaction between Co moments in the Co/Gd multilayer and the underlying SmCo overwhelms the Zeeman energy of the Gd moments, forcing the Gd moments to be antiparallel to the negative coercive field [see Fig. 4(b)]. The consequence is the reversal of the Gd aligned state of the multilayer before the magnetic field switches direction, as shown in Fig. 4(b).

The coercive field for the hard SmCo layer increases to over 2.5 kOe at 10 K nearly double the value for a single layer at the same temperature, as previously shown in Fig. 2. This too is a consequence of the antiferromagnetic coupling between the multilayer and the SmCo. To reverse the SmCo orientation requires domain wall creation between the SmCo and Co/Gd multilayers. This domain wall may be in the hard layer, in the soft Co/Gd multilayer, or where surface spins reorient and couple strongly to the SmCo layer. Domain wall creation due to the hard layer reversal for the exchange-coupled rare earth/transition metal double or triple layers is well documented.[45–57] Domain wall occurs since the Zeeman energy is larger at high fields in order to overcome the strong antiferromagnetic coupling. In other words, this is the reverse mechanism where the exchange spring behavior occurs at the reversal of the hard layer in the presence of an already oriented soft layer.

As shown in Fig. 4(a), the negative coercivity state persists as the temperature increases up to 150 K. Above 150 K, the system gradually changes the negative coercivity state first to a low coercivity (positive) state, then eventually to a more coercive state as the SmCo moment dominates the total moment at 200 K through compensation. One has to remember that $1/M_S$ dependent coercivity of the Co/Gd multilayer increases asymptotically around T_{comp} where the total magnetic moment goes to zero. Here, M_S denotes the net saturation magnetization. This is why the negative coercivity turns to positive close to and below T_{comp}. Above T_{comp}, the exchange spring mechanism leads to the observed maximum energy product with positive coercivity.

On the hysteresis loops shown in Figs. 4(a) and 4(b), at fields between the switching of the Co/Gd layer and the SmCo reversal, an exponential-type tail is observed between zero field and ±1 kOe on both sides of the hysteresis loop. The exponential tail may be due to the compression of the lateral domain wall commonly seen in exchange springs[58] and domain wall junctions.[48,59] However, this tail may also be attributed to a vortex state that becomes more prominent at low temperatures. When the field is reduced to zero, the entire multilayer has to reverse the magnetic direction in response to the (anti)ferromagnetic coupling between the SmCo and (Gd)Co. However, such reversals frequently induce magnetic vortices because of spin pinning at grain boundaries and edges. This is a well-known complication of Magnetic tunnel junctions, requiring careful shaping of the layer that is supposed to reverse. Micromagnetic studies[60–66] show that these vortices are very difficult to unwind. Clearly, the effect will be strongest when the boundary pinning is strongest, that is, at low temperatures. Although unlikely, we may alternatively attribute this tail to a multidomain state since the reversal of the Co/Gd multilayer may create a secondary domain wall at the interface if the initial domain wall formed at saturation does not relax with the reversal of the Co/Gd multilayer. It is also possible that the increasing external field may impose twisted states for the Co/Gd multilayer and further complicate the understanding.

Few studies on negative coercivity states can be found in the literature.[16,67–71] These can be classified into two groups. The first[67,68] found a negative coercivity state due to indirect exchange coupling through a nonmagnetic spacer when the coupling is antiferromagnetic. Such behavior vanishes when the coupling is made ferromagnetic by changing the spacer thickness. The second group of studies[16,69,70] observed inverted hysteresis loops (negative coercivity state) due to direct antiferromagnetic coupling in exchange-coupled bilayer or trilayer systems. A general understanding of such systems is still under debate. The observations in this paper fall into the second group in that we are able to tune the hard layer coercivity and thereby the negative coercivity state by controlling the Cu underlayer thickness. The results presented here are not accidental but rather demonstrate that the coercivity of the SmCo/(Co/Gd) system is tunable with negative and positive values at the fully antiferromagnetic state below T_{comp}.

To test the above mentioned results and to explore any changes when the interface between the SmCo and Co/Gd multilayers starts with the Co or Gd layer, we synthesized a (Co 35 Å/Gd 40 Å)$_{16}$/SmCo 300 Å/Cu 100 Å sample. The results are shown in Fig. 6. The hysteresis loop shapes and negative coercivity states are all retained (compared with Fig. 4) and are qualitatively independent of whether the Co/Gd multilayer on top of the SmCo layer starts with Co or Gd. However, at 10 K, in Fig. 6, the negative coercivity state becomes nearly zero unlike the values in Fig. 4. We will refer to this change and look for an explanation by calculating exchange constants later in the text. Therefore, when there is Gd at the interface of SmCo, it is the antiferromagnetic interfacial exchange coupling that works against the Zeeman energy at low external fields. Clearly, both the ferromagnetic coupling of SmCo with Co and the antiferromagnetic coupling of SmCo with Gd favor the same overall configuration for the combined SmCo/(Co/Gd) system in the Gd-aligned state at low external fields (when the Co/Gd multilayer switches direction), as shown in Figs. 4 and 6.

Exchange constants $J_{SmCo/Co}$ and $J_{SmCo/Gd}$ are calculated by equating the Zeeman energy of the multilayer (ML) magnetic moment in an applied magnetic field that is overcome by the interaction exchange energy gain upon aligning N spins at the interface,

$$2MVH = 2NJ\mathbf{S}_1 \cdot \mathbf{S}_2. \quad (1)$$

Here, M and V denote the net magnetization and volume of the ML, H is the (negative) field on the inverted loop, and J

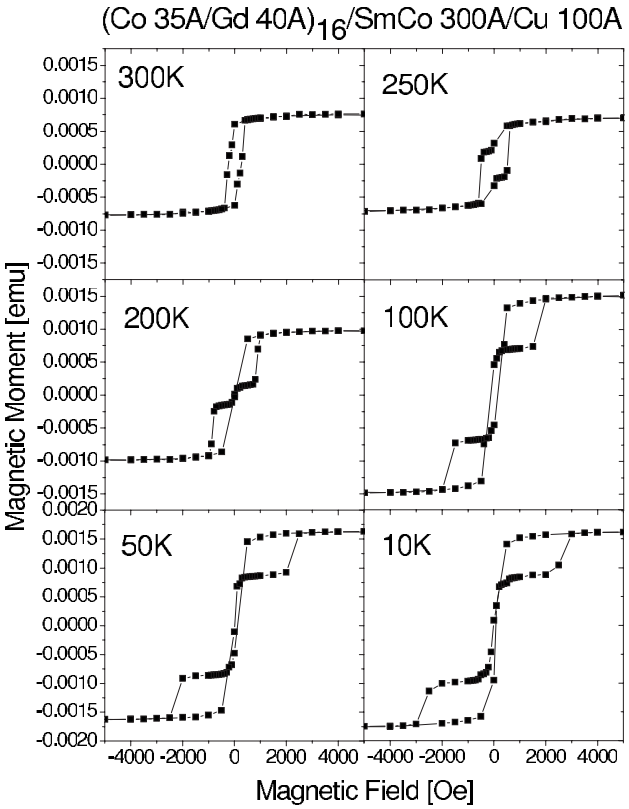

FIG. 6. Selected hysteresis loops as a function of temperature for the (Co 35 Å/Gd 40 Å)$_{16}$/SmCo 300 Å/Cu 100 Å system.

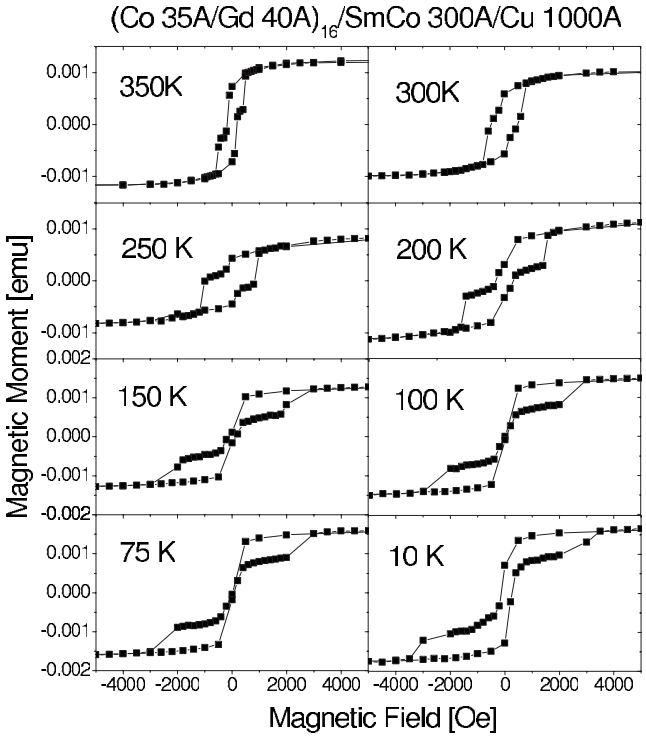

FIG. 7. Selected hysteresis loops as a function of temperature for the (Co 35 Å/Gd 40 Å)$_{16}$/SmCo 300 Å/Cu 1000 Å system.

and $\mathbf{S}_i$ are the effective exchange and spins at the ML/SmCo interface. We assume single-spin interactions across the interface. We use $H=-130$ Oe, the negative coercivity at 10 K seen in the inset to Fig. 4 and at 100 K in Fig. 6. The total saturation magnetization in the Gd-aligned state is $M_{\mathrm{Gd}}-M_{\mathrm{Co}}+M_{\mathrm{SmCo}}$. However, the SmCo magnetization does not switch direction when the Co/Gd multilayer reverses its direction at the negative coercive field, so the net magnetization rotation contributing to the Zeeman energy is $2(M_{\mathrm{Gd}}-M_{\mathrm{Co}})$ in the Gd-aligned state. We assume typical bulk values for $S_{\mathrm{Co}}=0.85$, $S_{\mathrm{Gd}}=3.5$ and find $(JS)_{\mathrm{SmCo/Co}}=0.62$ meV or $(JS)_{\mathrm{SmCo/Co}}/\mu_B=1.1\times10^5$ Oe and $(JS)_{\mathrm{SmCo/Gd}}=0.23$ meV or $(JS)_{\mathrm{SmCo/Gd}}/\mu_B=-4.0\times10^4$ Oe, in reasonable agreement with exchange values found for Co/Co and Co/Gd exchange interactions in literature.[27] The average spin for SmCo is $S_{\mathrm{SmCo}}=0.915$, so that, assuming that each ML spin interacts with only a single spin in the SmCo underlayer, the stated values are essentially the exchange energies. We have not included the anisotropy terms due to the lack of proper crystal structure. Although not obviously evident from Figs. 4 and 6, the negative coercivity appears to extend over a slightly larger temperature range for the Co-interfaced samples, perhaps reflecting the fact that $|J_{\mathrm{SmCo/Co}}|>|J_{\mathrm{SmCo/Gd}}|$. For the Co-interfaced film in Fig. 4, −130 Oe is observed at 10 K which is approximately 200 K below T_{comp}, whereas for the Gd interfaced film in Fig. 6, largest negative coercivity is observed at 100 K which is 150 K below T_{comp}. This comparison tends to indicate that the Co-interfaced system sustains the negative coercivity for a larger temperature interval than the Gd-interfaced system.

An explanation for the crossover of coercivity from negative to almost positive at 10 K in Fig. 6 can be understood through the characteristics of the multilayered ferrimagnets themselves. Normally, the ferrimagnets are soft materials due to the antiferromagnetically coupled interfaces and have coercivities on the order of 100 Oe or less at temperatures far below and far above T_{comp} (it is asymptotically high at T_{comp}). The coercivity of such a multilayer can also increase in the Gd-aligned state at temperatures far below T_{comp} when the Gd layer is sufficiently thick. That is to say, the middle of the Gd layers can act differently than those spins proximate to Co and this introduces twisted states into the system. These, in turn, have the effect of increasing the coercivity. Then, the effective ferrimagnetic Co/Gd system can be thought of ferri- + ferro- [(Co/Gd)/Gd] type where the single Gd layer is magnetically much harder than either of the Co or Co/Gd multilayer. Therefore, this explanation may be a good reason for the (Co 35 Å/Gd 40 Å)$_{16}$/SmCo 300 Å/Cu 100 Å multilayer (or any other multilayer ferrimagnet) to exhibit an extra anisotropy at Gd-aligned temperatures. This feature is well described in the literature.[43,72]

In Fig. 7, the temperature dependence of a similar (Gd 40 Å/Co 35 Å)$_{16}$/SmCo 300 Å/Cu 1000 Å multilayer is shown, where the coercivity of the SmCo layer is increased approximately 150 Oe due to the increased thickness of the Cu underlayer from 100 to 1000 Å. By doing so, as shown in Fig. 7, we could eliminate the negative coercivity state, although the system still remains in the fully antiferromagnetic state at relatively low positive coercive values be-

low T_{comp}. Therefore, the negative coercivity (inverted hysteresis loops) state is a function of the magnetic anisotropy of the system where one can turn it on and off, by regulating the coercivity of the hard layer in this case. The existence of higher coercivity indicates more grain boundaries and pinning sites which show resistance to the movement of SmCo domain walls inside the film. This may translate into the weaker interface coupling to the Co/Gd multilayer which prevents the negative coercivity in this case. Again at 10 K, we observe an additional coercivity increase consistent with the explanation for Fig. 6.

Comparing the hysteresis loops across T_{comp} from Figs. 4, 6, and 7, one can make a suggestion for the coercivity. The first observation is that the coercivity is larger for the soft phase above T_{comp} than below T_{comp} (exchange spring behavior of the soft layer). Likewise, the coercivity is larger for the hard phase below T_{comp} than it is above T_{comp} (exchange-spring-like behavior of the hard layer).

In conclusion, tunable coercivity is realized for the SmCo/(Co/Gd) systems below T_{comp}. A negative coercivity state arises in the Gd-aligned state when the interfacial coupling overwhelms the Zeeman energy at low external fields, at least for a sufficiently low coercivity SmCo magnet. Negative coercivity for the SmCo/(Co/Gd) system becomes positive when the coercivity of the hard layer or the soft layer increases depending on the ferrimagnetic characteristics of the systems. Although negative coercivity state is independent of whether there is Co or Gd in the proximity of the SmCo interface, negative coercivity is observed over a larger temperature interval for the more strongly coupled Co-interfaced multilayer.

The work at UTA is supported by a grant (No. Y-1215) from The Welch Foundation.

[1] J. M. D. Coey, Solid State Commun. **102**, 101 (1997).
[2] P. Campbell, *Permanent Magnet Materials and their Application* (Cambridge University Press, Cambridge, 1994).
[3] Y. Okumura, H. Fujimori, O. Suzuki, N. Hosoya, X. B. Yang, and H. Morita, IEEE Trans. Magn. **30**, 4038 (1994).
[4] S. S. Malhotra, Y. Liu, Z. S. Shan, S. H. Liou, D. C. Stafford, and D. J. Sellmayer, J. Appl. Phys. **79**, 5958 (1996).
[5] I. A. Al-Omari and D. J. Sellmyer, Phys. Rev. B **52**, 3441 (1995).
[6] M. Shindo, M. Ishizone, H. Kato, T. Miyazaki, and A. Sakuma, J. Magn. Magn. Mater. **161**, L1 (1996).
[7] K. Mibu, T. Nagahama, and T. Shinjo, J. Magn. Magn. Mater. **163**, 75 (1996).
[8] E. E. Fullerton, J. S. Jiang, M. Grimsditch, C. H. Sowers, and S. D. Bader, Phys. Rev. B **58**, 12193 (1998).
[9] R. J. Astalos and R. E. Camley, Phys. Rev. B **58**, 8646 (1998).
[10] S. Takei, A. Morisako, and M. Matsumoto, J. Appl. Phys. **87**, 6968 (2000).
[11] J. E. Davies, O. Hellwig, E. E. Fullerton, J. S. Jiang, S. D. Bader, G. T. Zimanyi, and K. Liu, Appl. Phys. Lett. **86**, 262503 (2005).
[12] E. Goto, N. Hayashi, T. Miyashita, and K. Nakagawa, J. Appl. Phys. **36**, 2951 (1965).
[13] E. F. Kneller and R. Hawig, IEEE Trans. Magn. **27**, 3588 (1991).
[14] R. Skomski and J. M. D. Coey, Phys. Rev. B **48**, 15812 (1993).
[15] M. Sawicki, G. J. Bowden, P. A. J. de Groot, B. D. Rainford, J.-M. L. Beaujour, R. C. C. Ward, and M. R. Wells, Phys. Rev. B **62**, 5817 (2000).
[16] K. Dumesnil, C. Dufour, Ph. Mangin, A. Rogalev, and F. Wilhelm, J. Phys.: Condens. Matter **17**, L215 (2005).
[17] R. E. Camley and D. R. Tilley, Phys. Rev. B **37**, 3413 (1988).
[18] R. E. Camley, Phys. Rev. B **39**, 12316 (1989).
[19] Y. Okumura, H. Fujimori, O. Suzuki, N. Hosoya, X. B. Yang, and H. Morita, IEEE Trans. Magn. **30**, 4038 (1994).
[20] G. Zangari, B. Lu, D. E. Laughlin, and D. N. Lambert, J. Appl. Phys. **85**, 5759 (1999).
[21] S. Takei, A. Morisako, and M. Matsumoto, J. Appl. Phys. **87**, 6968 (2000).
[22] J. Sayama, K. Mizutani, T. Asahi, J. Ariake, K. Ouchi, and T. Osaka, J. Magn. Magn. Mater. **301**, 271 (2006).
[23] A. Morisako, I. Kato, S. Takei, and X. Liu, J. Magn. Magn. Mater. **303**, e274 (2006).
[24] A. Morisako and X. Liu, J. Magn. Magn. Mater. **304**, 46 (2006).
[25] I. Kato, S. Takei, X. Liu, and A. Morisako, IEEE Trans. Magn. **42**, 2366 (2006).
[26] Y. K. Takahashi, T. Ohkubo, and K. Hono, J. Appl. Phys. **100**, 053913 (2006).
[27] S. Demirtas, M. R. Hossu, R. E. Camley, H. C. Mireles, and A. R. Koymen, Phys. Rev. B **72**, 184433 (2005).
[28] P. Chaudhari, J. J. Coumo, and R. J. Gambino, Appl. Phys. Lett. **22**, 337 (1973).
[29] T. Morishita, Y. Togami, and K. Tsushima, J. Phys. Soc. Jpn. **54**, 37 (1985).
[30] M. Mansuripur and M. F. Ruane, IEEE Trans. Magn. **22**, 33 (1986).
[31] M. Taborelli, R. Allenspach, G. Boffa, and M. Landolt, Phys. Rev. Lett. **56**, 2869 (1986).
[32] M. Takahashi, A. Yoshihara, T. Shimamori, T. Wakiyama, T. Miyazaki, K. Hayashi, and S. Yamaguchi, J. Magn. Magn. Mater. **75**, 252 (1988).
[33] D. J. Webb, A. F. Marshall, Z. Sun, T. H. Geballe, and R. M. White, IEEE Trans. Magn. **24**, 588 (1988).
[34] M. Sajieddine, Ph. Bauer, K. Cherifi, C. Dufour, G. Marchal, and R. E. Camley, Phys. Rev. B **49**, 8815 (1994).
[35] J. G. LePage and R. E. Camley, Phys. Rev. Lett. **65**, 1152 (1990).
[36] S. Uchiyama, Mater. Chem. Phys. **42**, 38 (1995).
[37] W. Hahn, M. Loewenhaupt, Y. Y. Huang, G. P. Felcher, and S. S. P. Parkin, Phys. Rev. B **52**, 16041 (1995).
[38] N. H. Duc and D. Givord, J. Magn. Magn. Mater. **157-158**, 169 (1996).
[39] D. Raasch and H. Wierenga, J. Magn. Magn. Mater. **168**, 336 (1997).
[40] J. Colino, J. P. Andrés, J. M. Riveiro, J. L. Martínez, C. Prieto, and J. L. Sacedón, Phys. Rev. B **60**, 6678 (1999).
[41] A. Koizumi, M. Takagaki, M. Suzuki, N. Kawamura, and N. Sakai, Phys. Rev. B **61**, R14909 (2000).

[42] D. Haskel, Y. Choi, D. R. Lee, J. C. Lang, G. Srajer, J. S. Jiang, and S. D. Bader, J. Appl. Phys. **93**, 6507 (2003).
[43] N. Hosoito, H. Hashizume, and N. Ishimatsu, J. Phys.: Condens. Matter **14**, 5289 (2002).
[44] S. Demirtas, R. E. Camley, and A. R. Koymen, Appl. Phys. Lett. **87**, 202111 (2005).
[45] S. Tsunashima, in *Magneto-optical Recording Materials*, edited by R. J. Gambino and T. Suzuki (IEEE, New Jersey, 2000).
[46] S. Becker, T. Lucinski, H. Rohrman, F. Stobiecki, and K. Roll, J. Magn. Magn. Mater. **140-144**, 521 (1995).
[47] M. Tabata, T. Kobayashi, S. Shiomi, and M. Masuda, Jpn. J. Appl. Phys., Part 1 **36**, 7177 (1997).
[48] S. Mangin, G. Marchal, and B. Barbara, Phys. Rev. Lett. **82**, 4336 (1999).
[49] R. Sbiaa and H. Le Gall, Appl. Phys. Lett. **75**, 256 (1999).
[50] M. Sawicki, G. J. Bowden, P. A. J. de Groot, B. D. Rainford, J. M. L. Beaujour, R. C. C. Ward, and M. R. Wells, Appl. Phys. Lett. **77**, 573 (2000).
[51] E. Stavrou, R. Sbiaa, T. Suzuki, and K. Roell, J. Appl. Phys. **87**, 6893 (2000).
[52] F. Canet, S. Mangin, C. Bellouard, and M. Piecuch, Europhys. Lett. **52**, 594 (2000).
[53] S. N. Gordeev, J.-M. L. Beaujour, G. J. Bowden, B. D. Rainford, P. A. J. de Groot, R. C. C. Ward, M. R. Wells, and A. G. M. Jansen, Phys. Rev. Lett. **87**, 186808 (2001).
[54] R. Morales, J. I. Martin, and J. M. Alameda, Phys. Rev. B **70**, 174440 (2004).
[55] K. Dumesnil, C. Dufour, Ph. Mangin, F. Wilhelm, and A. Rogalev, J. Appl. Phys. **95**, 6843 (2004).
[56] R. Morales, L. M. Alvarez-Prado, J. I. Martin, and J. M. Alameda, J. Magn. Magn. Mater. **272-276**, 1427 (2004).
[57] S. Demirtas and A. R. Koymen, J. Phys.: Condens. Matter **19**, 086230 (2007).
[58] A. Yu. Dobin and H. J. Richter, Appl. Phys. Lett. **89**, 062512 (2006).
[59] S. Mangin, C. Bellouard, S. Andrieu, F. Montaigne, P. Ohresser, N. B. Brookes, and B. Barbara, Phys. Rev. B **70**, 014401 (2004).
[60] R. P. Cowburn, D. K. Koltsov, A. O. Adeyeye, M. E. Welland, and D. M. Tricker, Phys. Rev. Lett. **83**, 1042 (1999).
[61] T. Shinjo, T. Okuno, R. Hassdorf, K. Shigeto, and T. Ono, Science **289**, 930 (2000).
[62] E. Girgis, J. Schelten, J. Shi, J. Janesky, S. Tehrani, and H. Goronkin, Appl. Phys. Lett. **76**, 3780 (2000).
[63] J. Shi, S. Tehrani, and M. R. Scheinfein, Appl. Phys. Lett. **76**, 2588 (2000).
[64] K. Yu. Guslienko, V. Novosad, Y. Otani, H. Shima, and K. Fukamichi, Phys. Rev. B **65**, 024414 (2001).
[65] M. Natali, I. L. Prejbeanu, A. Lebib, L. D. Buda, K. Ounadjela, and Y. Chen, Phys. Rev. Lett. **88**, 157203 (2002).
[66] V. Novosad, M. Grimsditch, K. Yu. Guslienko, P. Vavassori, Y. Otani, and S. D. Bader, Phys. Rev. B **66**, 052407 (2002).
[67] K. Takanashi, H. Kurokawa, and H. Fujimori, Appl. Phys. Lett. **63**, 1585 (1993).
[68] D. Y. Kim, C. G. Kim, C. O. Kim, S. S. Yoon, M. Naka, M. Tsunoda, and M. Takanashi, J. Magn. Magn. Mater. **304**, e356 (2006).
[69] D. Givord, J. Betz, K. Mackay, J. C. Toussaint, J. Vorion, and S. Wuchner, J. Magn. Magn. Mater. **159**, 71 (1996).
[70] S. M. Valvidares, L. M. Alverez-Prado, J. I. Martin, and J. M. Alameda, Phys. Rev. B **64**, 134423 (2001).
[71] S. Ohkoshi, T. Hozumi, and K. Hashimoto, Phys. Rev. B **64**, 132404 (2001).
[72] S. Demirtas, Ph.D. thesis, University of Texas at Arlington, 2005.